To cite this article: Chao Liang & Wei Ji (2011): On the Chord Length Sampling in 1-D Binary Stochastic Media, Transport Theory and Statistical Physics, 40:5, 282-303

To link to this article: http://dx.doi.org/10.1080/00411450.2011.639432

On the Chord Length Sampling in 1-D Binary Stochastic Media

Chao Liang and Wei Ji*

Department of Mechanical, Aerospace, and Nuclear Engineering

Rensselaer Polytechnic Institute, Troy, NY 12180-3590

**corresponding author: (518)-2766602 (telephone), (518)-2766025 (fax), jiw2@rpi.edu*

When the chord length sampling method is applied to solve radiation transport problems in random media where inclusions are randomly distributed in a background region, inaccuracy occurs due to two major factors: memory effect and boundary effect. In this paper, by applying chord length sampling to solve fixed source and eigenvalue problems in 1-D binary stochastic media, an investigation on how and why these two effects give rise to the inaccuracy in the final solutions is performed. The investigation is based on a series of radiation transport simulations for the calculation of reflection rate, flux distribution and effective multiplication factor.

KEYWORDS: chord length sampling, random media, radiation transport, Monte Carlo method, chord length probability distribution function

To cite this article: Chao Liang & Wei Ji (2011): On the Chord Length Sampling in 1-D Binary Stochastic Media, Transport Theory and Statistical Physics, 40:5, 282-303

To link to this article: http://dx.doi.org/10.1080/00411450.2011.639432

1. Introduction

Much work has been done to establish the chord length sampling (CLS) method as an acceptable modeling technique over the past two decades since it was first proposed by Zimmerman and Adams (1991). In their original paper, a transmission problem was simulated in a finite 1-D binary stochastic medium, where two materials are alternately distributed. The thickness of each material follows an exponential distribution. CLS is performed to sample the distance to the next material interface each time a neutron scatters in one material or crosses a material interface. This sampling is based on a chord length probability density function (PDF), which is the material thickness distribution function. Zimmerman and Adams proposed three algorithms in performing CLS, depending on whether the material interface is remembered or not when a backscattering event happens in one material. Later, many researchers have followed this original work and applied CLS to solve different transport problems in different geometry configurations. Brantley (2011) followed and extended Zimmerman and Adams' original work to calculate average flux distribution in the same 1-D geometry and compared the accuracy of the first two algorithms. Murata et al. (1996, 1997) applied empirical nearest neighbor distribution functions (NNDs) to sample chord length to the next TRISO particles in the analysis of high temperature gas cooled reactors and excellent results were obtained in criticality calculations. Donovan and Danon (2003) and Donovan et al. (2003) systematically investigated the application of CLS to 2-D/3-D geometry for fixed source problems and proposed an empirical method to determine the chord length PDF. Ji and Martin (2007a, 2008) used a theoretical chord length distribution function to validate application of CLS in a general 3-D geometry and developed a self-consistent correction algorithm to obtain an effective total volume packing fraction used in CLS to analyze Very High Temperature Reactor (VHTR) unit cells. More recently, Reinert et al. (2010) incorporated CLS into a hybrid methodology framework in solving transport problems involving randomly densely packed, optically thick absorber systems.

Although CLS was originally proposed to be used in both materials each time the distance to the material interface is sampled (Zimmerman and Adams, 1991), in practice, CLS is used only in a background material to sample the next inclusion material while regular Monte Carlo is used in the inclusion material, such as disks in 2-D (Donovan and Danon, 2003) and spheres in 3-D (Murata et al., 1996 and 1997; Ji and Martin, 2007a and 2008; Reinert et al., 2010). In these applications, the system is finite and fixed-size inclusions are uniformly distributed in a background material region. When CLS is applied to analyze neutronic behavior in such geometry, some complications exist to cause inaccurate solutions compared to Monte Carlo

To cite this article: Chao Liang & Wei Ji (2011): On the Chord Length Sampling in 1-D Binary Stochastic Media, Transport Theory and Statistical Physics, 40:5, 282-303

To link to this article: http://dx.doi.org/10.1080/00411450.2011.639432

benchmark simulations. Major factors that give rise to the inaccuracy are rooted in the CLS procedure itself. When a neutron leaves an inclusion and scatters back, should a new inclusion be sampled or should the old one be remembered? This poses a memory effect issue in the CLS method. The other effect is boundary effect. When sampled inclusion is overlapped with an external boundary, it is rejected and a re-sampling is performed. This would result in non-uniform distribution of inclusions in background material and affect neutron spatial distributions. How these two effects affect the CLS accuracy has not yet been thoroughly investigated.

In the current work, by applying CLS to radiation transport in finite 1-D random media with uniformly distributed inclusions for fixed source and eigenvalue problems, we studied memory and boundary effects by calculating reflection rate, effective multiplication factor and flux distribution.

2. Radiation Transport in Finite 1-D Stochastic Geometry

A finite 1-D stochastic configuration is set up for Monte Carlo benchmark computations. In this configuration, a certain number of fixed-width inclusions are uniformly and randomly distributed in the background material region with the total length of L. Each inclusion has the same material which is different from the background material. In the Monte Carlo benchmark computation for fixed-source and eigenvalue problems, both transport simulations are performed on each physical realization of the configuration and the predicted reflecting probability, effective multiplication factor and flux distribution are averaged over large numbers of realizations.

In each physical realization, the random configuration is constructed by placing the center of each inclusion at a randomly sampled position within [t/2, L-t /2], where t is the thickness of the inclusion. If there is an overlap with the existing inclusions, the sampled inclusion is rejected and a new one is sampled. This process is typically called Random Sequential Addition (RSA) (Widom, 1966). The construction is performed until the total number of inclusions generated meets the predetermined criterion. Normally, the total volume packing fraction of the inclusion is used as a criterion. It is defined as the ratio of the total volume of inclusions and the total volume of the system, and denoted as *frac*. In 1-D stochastic geometry, *frac*=N*t/L, where N is the total number of inclusions. A typical realization configuration is shown in Figure 1.

To cite this article: Chao Liang & Wei Ji (2011): On the Chord Length Sampling in 1-D Binary Stochastic Media, Transport Theory and Statistical Physics, 40:5, 282-303

To link to this article: http://dx.doi.org/10.1080/00411450.2011.639432

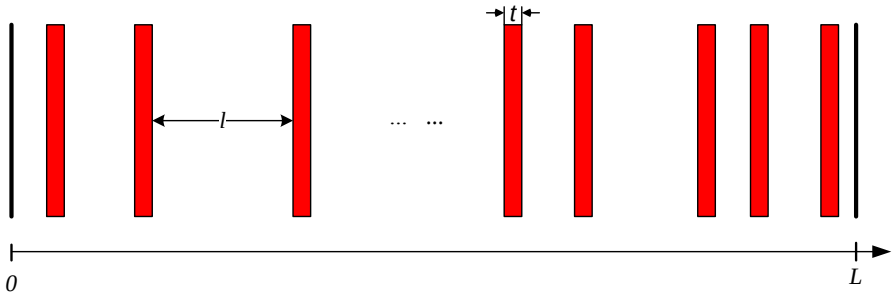

FIGURE 1 Benchmark configuration of 1-D binary stochastic media: inclusions with thickness *t* are uniformly placed one by one without overlap in the slab geometry with the length *L*.

When the CLS method is applied to solving the radiation transport problem in the 1-D stochastic geometry as described above, CLS is performed only in the background material region while a regular Monte Carlo procedure is performed in the inclusions. Each time a neutron leaves an inclusion or scatters in the background region, the distance to the next inclusion and the distance to the collision site are sampled. The neutron is advanced to the new location depending on which distance is smaller. Thus, inclusions are sampled on the fly during a neutron's random walk process without explicitly modeling the locations of all the inclusions, which greatly decreases the simulation time and mitigates the memory requirement. Multiple simulations on different physical realizations can be transformed to only one simulation based on an on-the-fly sampling process.

Each time the CLS is performed, a chord length PDF is used to sample the next inclusion. It has been shown that this PDF is well approximated by an exponential function with the form (Ji and Martin, 2008; Griesheimer et al., 2011; Torquato, 2002):

$$f(l) = \frac{1}{< l >} \exp(-\frac{l}{< l >}), \tag{1}$$

where l is the chord length between two adjacent inclusions, and $<l>$ is the mean chord length. In 1-D, the mean chord length is expressed by:

$$< l >= \frac{1 - frac}{frac} t. \tag{2}$$

It should be emphasized that Eq. (1) is derived for the chord length distribution in an infinite medium and is very accurate under the conditions of $t<<L$ and small *frac*. To verify the accuracy of Eq. (1), a large 1-D stochastic configuration with L=1000cm and t=0.1cm is modeled to represent infinite medium as shown in Figure 1. Periodic boundary conditions are applied on both sides. The real chord length distribution is calculated based on 10^{12} chord lengths tallied between

To cite this article: Chao Liang & Wei Ji (2011): On the Chord Length Sampling in 1-D Binary Stochastic Media, Transport Theory and Statistical Physics, 40:5, 282-303

To link to this article: http://dx.doi.org/10.1080/00411450.2011.639432

inclusions over 10^9 physical realizations at the packing fraction of 10%. The cumulative distribution functions (CDFs) of both analytical and empirical results are shown in Figure 2 and excellent agreement is obtained.

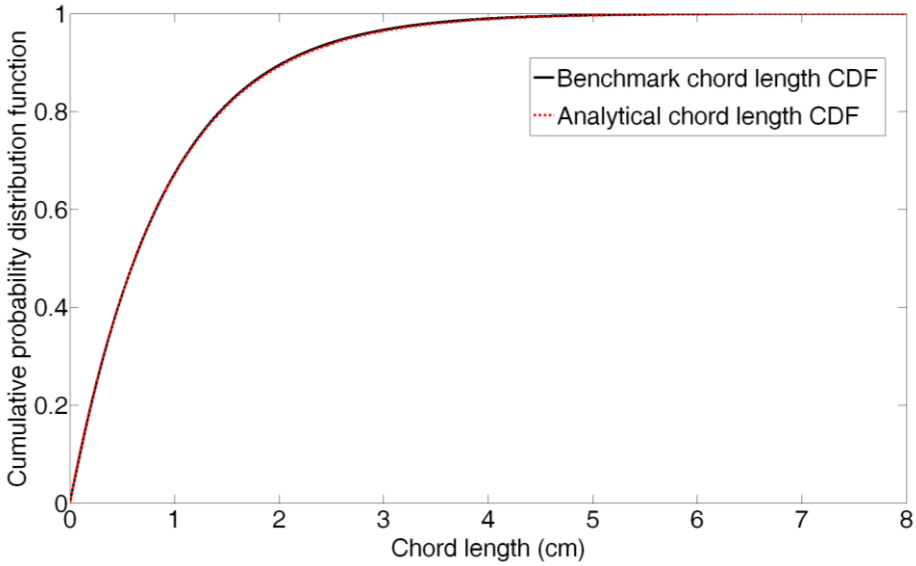

FIGURE 2 Cumulative distribution functions of chord lengths between two inclusions: real distribution in benchmark configuration vs. theoretical distribution in a derived function

In our investigation of performing CLS in finite 1-D geometry, Eq. (1) is used to sample the next inclusion when 1) a neutron enters the stochastic medium through the external boundary; 2) a neutron leaves an inclusion; 3) a neutron scatters in the background material. Previous research has shown that in either case, the chord length distribution is the same in 1-D geometry, and can be well approximated by Eq. (1) (Griesheimer et al., 2011; Ji and Martin, 2007b). In the current work, we use the same chord length PDF in the CLS method.

Due to the finite size of the system, each time a new inclusion is sampled by CLS, it could overlap with the external boundary of the system. If the sampled collision distance is longer than the sampled distance to the new inclusion, the neutron should advance to the new inclusion that is partially clipped by the external boundary. This is not physically realistic (at least in the benchmark configuration). The sampled new inclusion should be rejected and re-sampled. Thus, the distribution of inclusions produced by the CLS procedure in the system will not be uniform due to this re-sampling, at least in the region near the external boundary. While in the benchmark configuration, it is uniform over the whole domain. Such a complication can result in different neutron behaviors at the region near the boundary and may affect the overall flux distribution

To cite this article: Chao Liang & Wei Ji (2011): On the Chord Length Sampling in 1-D Binary Stochastic Media, Transport Theory and Statistical Physics, 40:5, 282-303

To link to this article: http://dx.doi.org/10.1080/00411450.2011.639432

compared to the benchmark computation. This effect is due to the overlap between the sampled inclusion and the system boundary, which we define as "boundary effect". How the boundary effect affects the accuracy of the CLS method is one of the major research issues that will be addressed in this paper.

Another phenomenon observed in the CLS procedure is about backscattering events. When a neutron leaves an inclusion, the next subsequent CLS procedure may end up with a scattering event in the background region. If the neutron scatters back and flies towards the inclusion it has just left, it could enter the inclusion without any collision in the background. At this point, a similar dilemma exists as the one encountered in the original work done by Zimmerman and Adam (1991). In their work, depending on whether the neutron should or should not remember the interface between the two materials, three algorithms were proposed in the CLS procedure and it showed that remembering the interface can improve the accuracy. We may define this effect as "memory effect". However, in the current work, the random medium benchmark configuration is different from the geometry in Zimmerman and Adam's work. In the current work, the random media are constructed by placing fixed-thickness inclusions (material 1) randomly in the background region (material 2), while in Zimmerman and Adams' original work, inclusions of material 1 and 2 are placed alternately with random thicknesses that follow exponential distributions. A question naturally arises: whether the CLS accuracy can be improved by remembering the last inclusion the neutron has just left in the scope of the current work? How the memory effect affects the accuracy of the CLS method is another major research issue that will be addressed in this paper.

In the following sections, we first investigate the boundary effect by applying CLS to a radiation transport problem in a vacuum binary random medium. The local volume packing fraction distribution of inclusions is computed to demonstrate how the boundary effect changes the distribution of inclusions. Next, both the boundary and memory effects are investigated by applying CLS to solving two typical transport problems: a fixed source problem and an eigenvalue problem. Finally, conclusions are provided.

3. Analysis of Boundary Effect in Vacuum Random Medium

To have a better understanding of the CLS procedure and the associated boundary effect, we construct a vacuum binary random medium to study the CLS and its boundary effect. The constructed configuration is the same as the benchmark configuration shown in Figure 1 but the background and inclusion materials are vacuum materials. Assuming a beam of neutrons incident on the left, we apply CLS to simulate the neutron transport process. Since the system is vacuum,

To cite this article: Chao Liang & Wei Ji (2011): On the Chord Length Sampling in 1-D Binary Stochastic Media, Transport Theory and Statistical Physics, 40:5, 282-303

To link to this article: http://dx.doi.org/10.1080/00411450.2011.639432

all the neutrons will penetrate the background material and inclusion material alternately in the system and leak out from the right boundary. Figure 3 shows a neutron history from left to right. The distance from one inclusion to the next inclusion l_i, is sampled from Eq. (1).

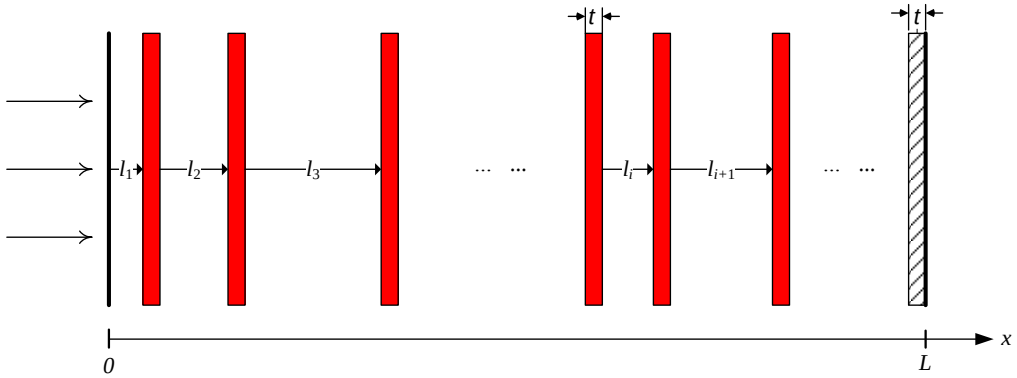

FIGURE 3 Configuration and sampling procedure in 1-D system: inclusions are sampled on the fly as the radiation particles penetrate the system from left to right.

Instead of predicting any neutronic behavior, we record the sampled inclusions' locations during each neutron history and calculate the inclusion's local volume packing fraction as a function of location in the 1-D system. Due to re-sampling if a sampled inclusion is overlapped with the boundary in the CLS method, as noted in the shadowed forbidden region of Figure 3, the inclusion distribution in the CLS simulation can be quite different from the benchmark configuration, which is exactly uniform distribution. To study this difference, a 1-D system with the total length of 200cm is set up to perform the above simulation. The thickness of the inclusion is 0.1cm and the total volume packing fraction of the inclusion is 10%. A total of 20,000 meshes are used with a mesh width of 0.01cm. If the sampled inclusion is located in a mesh, the actual volume of the inclusion that falls inside each mesh is accumulated. A total of 10^9 neutron histories are tracked and the local volume packing fraction in each mesh is averaged to per neutron history. Meanwhile, to make a comparison with the benchmark configuration, we also compute the local packing fraction of inclusions with the same mesh bins by averaging over 100 physical realizations. Both the CLS and the benchmark simulation results are shown in Figure 4.

To cite this article: Chao Liang & Wei Ji (2011): On the Chord Length Sampling in 1-D Binary Stochastic Media, Transport Theory and Statistical Physics, 40:5, 282-303

To link to this article: http://dx.doi.org/10.1080/00411450.2011.639432

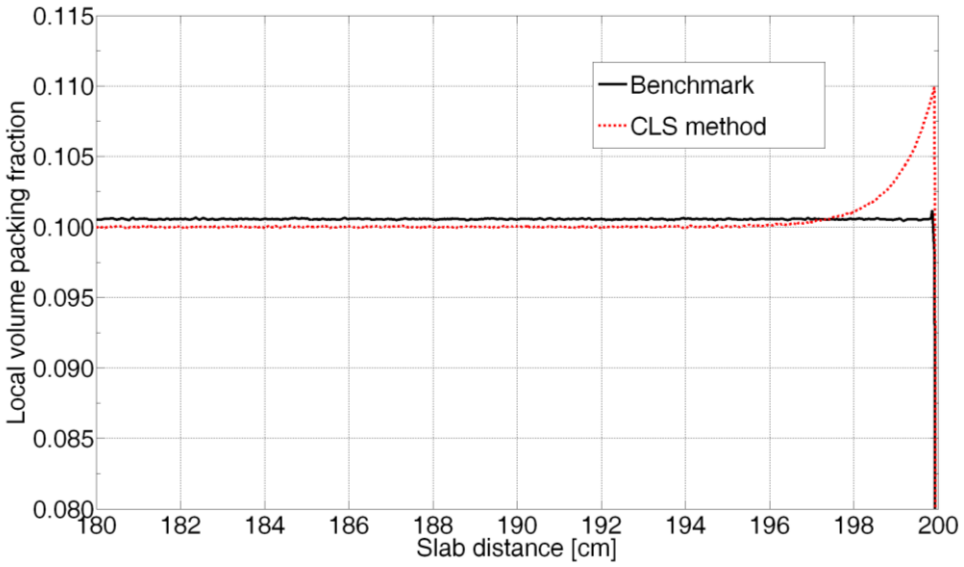

FIGURE 4 Spatial distribution of the local volume packing fraction of the inclusion in 1-D system

To better present the significant differences, we show the local packing fractions only at the region near the right boundary. The rest of region has the same flat distribution as the beginning region in the plot. It can be seen that in most regions, CLS presents 10% local packing fraction, which is consistent with the nominal total volume packing fraction of 10%. At the region near the boundary (from 196cm to 199.9cm), local packing fraction starts increasing to the value of 11%. After that, it drops linearly to zero at the boundary. The increase in the packing fraction is due to the re-sampling process, which increases the probability that inclusions would appear at the region about 40 inclusion thicknesses away from the boundary. Due to the forbidden region, which is one thickness width from the boundary, the packing fraction abruptly decreases to zero within a short distance of 199.9cm to 200cm. The total volume packing fraction in the CLS simulation can be calculated by the integration of the local volume packing fraction over the system divided by the total length. Although a higher inclusion density appears near the boundary, the total volume packing fraction of the inclusion in the CLS simulation is still less than but close to the nominal total packing fraction of 10% in the benchmark configuration. Our calculation shows a 9.9997% total packing fraction in the CLS simulation. This is a natural result of not allowing the overlapping, which effectively decreases the total amount of inclusion materials inside the system, even though resampling is applied. As a comparison, it is interesting to see that in the benchmark configuration, local packing fraction is constant in most regions with a value of about 10.06%, which is slightly higher than 10%. The same phenomenon appears for the benchmark configuration as the CLS case in the forbidden region: a sharp decrease to zero within

To cite this article: Chao Liang & Wei Ji (2011): On the Chord Length Sampling in 1-D Binary Stochastic Media, Transport Theory and Statistical Physics, 40:5, 282-303

To link to this article: http://dx.doi.org/10.1080/00411450.2011.639432

a short distance of 199.9cm to 200cm. This is due to the fact that the benchmark configuration is constructed by setting inclusions' centers only within the range of [0.05cm, 199.95cm] in the simulation. It results in a little higher inclusion density (10.06%) but the inclusions are still in a uniform distribution in the bulk of the system.

4. Fixed Source Problem in 1-D Stochastic Geometry

To investigate boundary and memory effects, fixed-source problems in 1-D stochastic geometry are simulated at different total packing fractions. The impact of two effects on the accuracy of CLS method is analyzed respectively by comparing the CLS results with the Monte Carlo benchmark results. In fixed-source problems, a unidirectional beam of neutrons is incident on a slab geometry system, which is configured as Figure 1. The total length of the system is 200cm and the thickness of the inclusion is 0.1cm. In this system, some neutrons may reflect back and leak out of system from the incident boundary. Some may penetrate the system and leak out from the other side or be absorbed in the system. The radiation reflection probability and flux distribution at fine spatial resolution (20,000 meshes with the mesh bin width of 0.01 cm) are computed in the simulations. Comparisons are made between Monte Carlo benchmark results and CLS results for a series of scenarios. These scenarios include different total volume packing fraction of inclusions, different cross section data for inclusion material, and with or without memory effect in CLS procedure. Table 1 summarizes these scenarios and lists the values of parameters used for the simulations.

To observe appreciable impacts from the memory and boundary effects, transport problems are designed so that neutrons would experience more scattering events in the system. In our study, cross sections of both background and inclusion materials are selected so that the mean free path in the background material is about the same order as the mean chord length in the background region between two inclusions. Only the inclusion material has slight absorption. Background material is a purely scattering material with a total cross section of 1.0cm^{-1}. This gives a mean free path of 1.0cm. Two sets of cross sections are selected for inclusion material, one has a low scattering cross section and the other has a high scattering cross section.

In the benchmark simulation, the conventional Monte Carlo procedure is performed over a total of 1,000 physical realizations. In each realization, a total of 10^4 neutron histories are tracked and the ensemble-averaged solutions are obtained over 1,000 realizations.

In the CLS simulation, when a neutron leaves an inclusion, if the inclusion is not removed from memory until the neutron enters another inclusion, it is denoted as "CLS w/ memory" method. Otherwise, it is the "CLS w/o memory" method. With memory, a neutron may enter the

To cite this article: Chao Liang & Wei Ji (2011): On the Chord Length Sampling in 1-D Binary Stochastic Media, Transport Theory and Statistical Physics, 40:5, 282-303

To link to this article: http://dx.doi.org/10.1080/00411450.2011.639432

same inclusion multiple times by backscattering events that happen in the background material. Both methods are examined and results are compared. The chord length PDF given by Eq. (1) is used for the chord length sampling. A total of 10^7 neutron particles are tracked in the CLS simulations.

TABLE 1 Comparison between CLS (w/ and w/o memory) and Monte Carlo benchmark solutions for fixed-source problems

(Background) $\Sigma_{t,1}$=1.0cm^{-1}, $\Sigma_{a,1}$=0cm^{-1}, $\Sigma_{s,1}$=1.0cm^{-1}				
t=0.1cm, L=200cm	(Inclusion) $\Sigma_{t,2}$=0.1cm^{-1}, $\Sigma_{a,2}$=0.05cm^{-1}, $\Sigma_{s,2}$=0.05cm^{-1}		(Inclusion) $\Sigma_{t,2}$=10cm^{-1}, $\Sigma_{a,2}$=0.05cm^{-1}, $\Sigma_{s,2}$=9.95cm^{-1}	
Solution Method	Reflection Probability	Relative Error	Reflection Probability	Relative Error
frac=5%				
Benchmark	0.866±0.001		0.893±0.001	
CLS w/o memory	0.865±0.001	**-0.11%**	0.881±0.001	**-1.34%**
CLS w/ memory	0.837±0.001	**-3.35%**	0.856±0.001	**-4.14%**
frac=10%				
Benchmark	0.814±0.001		0.866±0.001	
CLS w/o memory	0.811±0.001	**-0.37%**	0.851±0.001	**-1.73%**
CLS w/ memory	0.789±0.001	**-3.07%**	0.832±0.001	**-3.93%**
frac=15%				
Benchmark	0.771±0.001		0.853±0.001	
CLS w/o memory	0.769±0.001	**-0.26%**	0.834±0.001	**-2.23%**
CLS w/ memory	0.751±0.001	**-2.59%**	0.821±0.001	**-3.75%**
frac=20%				
Benchmark	0.736±0.001		0.845±0.001	
CLS w/o memory	0.734±0.001	**-0.27%**	0.824±0.001	**-2.49%**
CLS w/ memory	0.718±0.001	**-2.45%**	0.814±0.001	**-3.67%**
frac=25%				
Benchmark	0.704±0.001		0.839±0.001	
CLS w/o memory	0.701±0.001	**-0.43%**	0.817±0.001	**-2.62%**
CLS w/ memory	0.688±0.001	**-2.27%**	0.809±0.001	**-3.58%**
frac=30%				
Benchmark	0.673±0.001		0.835±0.001	
CLS w/o memory	0.671±0.001	**-0.30%**	0.812±0.001	**-2.75%**
CLS w/ memory	0.660±0.001	**-1.93%**	0.807±0.001	**-3.35%**

Table 1 summarizes the results of the reflection probability at the total volume packing fractions ranging from 5% to 30%. It is shown that the CLS w/o memory produces better agreement with the benchmark than the CLS w/ memory. This phenomenon systematically exists under different packing fractions and cross section data, with better accuracy obtained at the case

To cite this article: Chao Liang & Wei Ji (2011): On the Chord Length Sampling in 1-D Binary Stochastic Media, Transport Theory and Statistical Physics, 40:5, 282-303

To link to this article: http://dx.doi.org/10.1080/00411450.2011.639432

of lower packing fractions. The better accuracy obtained by the CLS w/o memory method can be explained by comparing with Zimmerman and Adams's "Algorithm B and C" (Zimmerman and Adams, 1991), where retaining memory improves the accuracy. In their work, the benchmark configuration is constructed by alternately generating binary stochastic media. The thickness of each material is sampled from predetermined exponential distribution functions, which are also the chord length PDFs used in CLS. When CLS is applied to solving the benchmark problem, chord lengths sampled from these PDFs are the distances from material interface to material interface, which are exactly the thicknesses that are generated in the benchmark configuration construction. If neutrons always cross material interfaces without any scattering in either material during the transport process, CLS can produce the exact results as the benchmark. However, if neutrons scatter in either material, the distance from the scattering site to the material interface will not follow an exponential distribution described by the chord length PDFs. If one still uses the same PDFs to sample the distance to the next material interface and as the CLS simulation process proceeds, the thickness of either material will no longer follow the same distributions as the benchmark configuration. Thus, it causes inaccuracy, which is demonstrated by "Algorithm A" in Zimmerman and Adam's work. The above discussion also explains why remembering the material interfaces can improve accuracy, which is demonstrated in "Algorithms B and C". In the current work, the benchmark configuration is different from Zimmerman and Adam's. It is constructed by uniformly placing fixed-thickness inclusions in the background material region. This construction process results in not only the distances between two inclusions, but also the distances from any point inside the background to the adjacent inclusion, will closely follow the exponential distribution (Ji and Martin, 2007b), which is expressed by Eq. (1). When this chord length PDF is used by CLS to simulate radiation transport, distances to the next inclusion are sampled whenever a neutron leaves an inclusion or scatters in the background material region, even if a back-scattering event happens. In this way, the statistical characteristics of the chord lengths generated by CLS procedure can be consistent with the benchmark configuration. Thus, the accuracy is kept. If the last inclusion is remembered and the backscattered neutron can travel to the remembered inclusion without a collision, this actually forces one to accept a specific chord length, which is not sampled from the exponential chord length PDF. Thus a non-exponential chord length distribution is produced by CLS w/ memory procedure, which is not consistent with the benchmark configuration. This is why CLS w/o memory shows better accuracy in the current work.

It is interesting to find that as the volume packing fraction increases from low to high, the CLS w/o memory method tends to increase the relative errors while the CLS w/ memory method

To cite this article: Chao Liang & Wei Ji (2011): On the Chord Length Sampling in 1-D Binary Stochastic Media, Transport Theory and Statistical Physics, 40:5, 282-303

To link to this article: http://dx.doi.org/10.1080/00411450.2011.639432

tends to decrease the relative errors. This is because the mean distance between adjacent inclusions (also called mean chord length of the background material) becomes smaller. Neutrons tend to pass through the background without a collision, so the backscattering events happen less frequently. Such a trend will make the difference between CLS w/o memory and CLS w/ memory smaller as shown in Table 1.

Boundary effect can also be observed from the results in Table 1. When the scattering cross section in the inclusion is increased by a factor of about 200, the relative errors between CLS w/o memory and benchmark solutions increase by a factor of 2 to 10. This considerable increase in the relative error can be explained by the boundary effect. In the fixed-source problems with the incoming unidirectional neutron beam, due to the scattering in the system, most neutrons will be reflected and leak out of the system. When neutrons try to leak out of the left boundary, if re-sampling happens, according to the analysis in Section 3, neutrons will "see" more densely distributed inclusions near the boundary. So neutrons have higher probability to be scattered back again into the system, or to be absorbed in the inclusions, than in the benchmark system, where inclusions are uniformly distributed near the boundary. This causes fewer neutrons to leak out of the left boundary in the CLS method compared to the benchmark. If the scattering cross section is higher, such as the high scattering cross section case studied here, the boundary effect is more significant. This is why CLS w/o memory solutions (reflection rates) are less than benchmark solutions with relative errors -1.34%~-2.75%. In general, boundary effect becomes significant when inclusions have highly scattering material.

Comparison of the flux distribution between CLS and benchmark can also demonstrate the memory and boundary effects on the accuracy. Figure 5 shows the spatial flux distributions obtained by the Monte Carlo benchmark, CLS w/o memory, and CLS w/ memory methods at the total volume packing fraction of 10%. Figure 5 (a) shows the results for the low scattering cross section case in the inclusion and (b) for the high scattering cross section case. It can be seen that most neutrons are distributed within a range of 0-50cm due to scattering in the system. To show this major feature, we plot the flux distribution only for the first 45cm and 35cm regions in (a) and (b) respectively. In both cases, generally speaking, the agreement between CLS w/o memory and benchmark is much better than CLS w/ memory. This again demonstrates that CLS w/o memory method gives more accurate solutions. Moreover, in the case of high scattering cross section, due to the boundary effect, more neutrons experience scattering interactions at the region near the left boundary and are reflected back into the deeper region of the system. This explains why higher flux is obtained by the CLS w/o memory method in Figure 5(b). When the inclusion scattering cross section is low, no appreciable deviation is obtained, as shown in Figure 5(a).

To cite this article: Chao Liang & Wei Ji (2011): On the Chord Length Sampling in 1-D Binary Stochastic Media, Transport Theory and Statistical Physics, 40:5, 282-303

To link to this article: http://dx.doi.org/10.1080/00411450.2011.639432

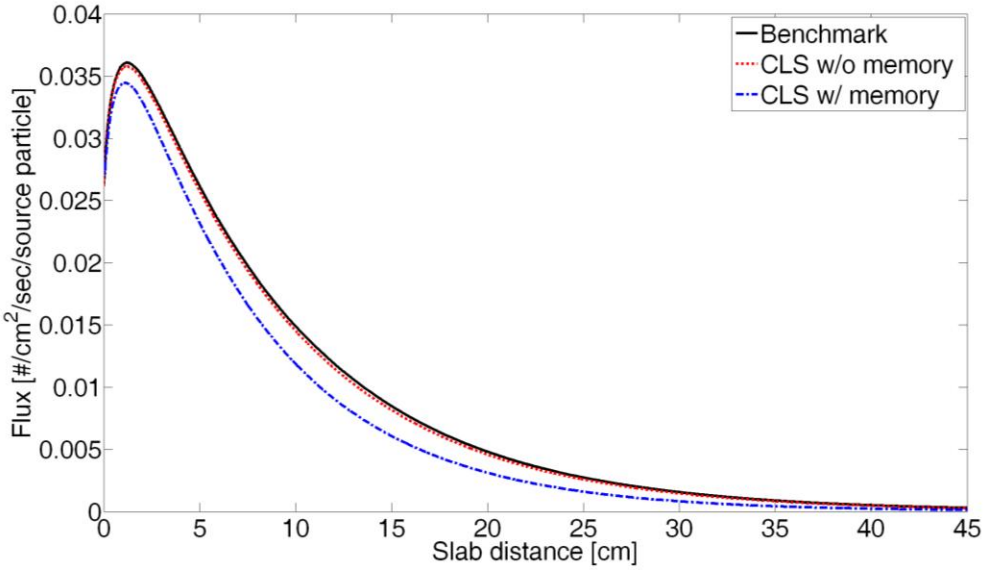

(a) Flux distribution in the system with low scattering cross section in inclusions

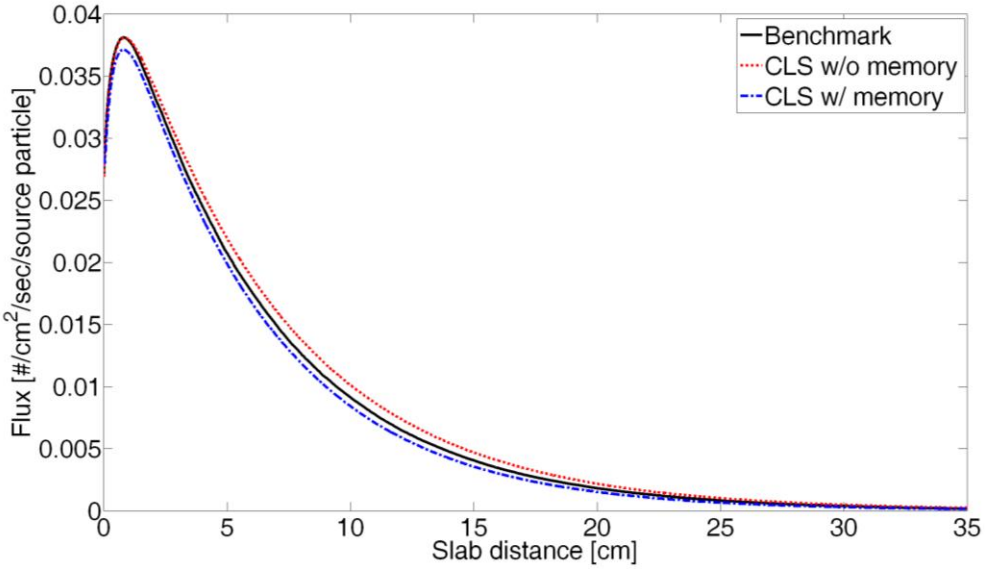

(b) Flux distribution in the system with high scattering cross section in inclusions

FIGURE 5 Flux distribution comparisons between Monte Carlo benchmark and CLS methods

5. Eigenvalue Problem in 1-D Stochastic Geometry

To investigate the boundary and memory effects, eigenvalue problems are simulated using Monte Carlo benchmark and CLS methods. In these problems, fission materials are included in the inclusions while the background is still pure scattering material. The benchmark configuration construction process is the same as the fixed-source problem. Effective multiplication factors k_{eff}

To cite this article: Chao Liang & Wei Ji (2011): On the Chord Length Sampling in 1-D Binary Stochastic Media, Transport Theory and Statistical Physics, 40:5, 282-303

To link to this article: http://dx.doi.org/10.1080/00411450.2011.639432

and neutron flux distribution are calculated. Four sets of cross section data are used to perform the simulations. These are shown in Table 2.

TABLE 2 Parameters in eigenvalue problem simulations

(t/L=5e-4)	Background (L=200cm)			Inclusion (10% packing fraction, t=0.1cm)				
Case	$\Sigma_{t,1}$	$\Sigma_{a,1}$	$\Sigma_{s,1}$	$\Sigma_{t,2}$	$\Sigma_{a,2}$	$\Sigma_{s,2}$	$\Sigma_{f,2}$	$\nu\Sigma_{f,2}$
1	$0.1cm^{-1}$	0	$0.1cm^{-1}$	$0.1cm^{-1}$	$0.05cm^{-1}$	$0.05cm^{-1}$	$0.02cm^{-1}$	$0.05cm^{-1}$
2	$0.1cm^{-1}$	0	$0.1cm^{-1}$	$10cm^{-1}$	$0.05cm^{-1}$	$9.95cm^{-1}$	$0.02cm^{-1}$	$0.05cm^{-1}$
3	$1cm^{-1}$	0	$1cm^{-1}$	$0.1cm^{-1}$	$0.05cm^{-1}$	$0.05cm^{-1}$	$0.02cm^{-1}$	$0.05cm^{-1}$
4	$1cm^{-1}$	0	$1cm^{-1}$	$10cm^{-1}$	$0.05cm^{-1}$	$9.95cm^{-1}$	$0.02cm^{-1}$	$0.05cm^{-1}$

In the Monte Carlo benchmark simulations, ensemble-averaged solutions (both effective multiplication factor and flux distribution) are obtained over 1000 realizations. In each realization, a total of 300 fission generations with 200 inactive generations are simulated with 10^4 neutron histories in each generation. In CLS simulations, a total of 300 generations with 200 inactive generations are performed with 10^6 initial neutron sources in each generation. To calculate the flux distribution, the slab is divided evenly into 20,000 bins and track length estimator is used to tally volume average flux in each bin. The relative standard deviation of the tallied flux in each bin is kept within 1% in the Monte Carlo benchmark simulation and within 0.1% in the CLS simulation.

TABLE 3 Comparison of effective multiplication factors between MC benchmark and CLS methods

Case	Benchmark	CLS w/o memory		CLS w/ memory	
	k_{eff}	k_{eff}	Relative error	k_{eff}	Relative error
1	0.8755±0.0001	0.8751±0.0001	-0.10%	0.8790±0.0001	0.40%
2	0.9853±0.0001	0.9790±0.0001	-0.64%	0.9780±0.0001	-0.74%
3	0.9825±0.0001	0.9824±0.0001	-0.01%	0.9871±0.0001	0.47%
4	0.9915±0.0001	0.9899±0.0001	-0.16%	0.9919±0.0001	0.04%

The comparison of the effective multiplication factor and the neutron flux distribution between the Monte Carlo benchmark and CLS methods are shown in Table 3 and Figure 6. It can be seen that both CLS w/o memory and CLS w/ memory methods can predict k_{eff} accurately. There are no considerable differences in the results between two CLS methods so the memory effect can be considered negligible. This is due to the fact that k_{eff} is more sensitive to the mass

To cite this article: Chao Liang & Wei Ji (2011): On the Chord Length Sampling in 1-D Binary Stochastic Media, Transport Theory and Statistical Physics, 40:5, 282-303

To link to this article: http://dx.doi.org/10.1080/00411450.2011.639432

conservation than the spatial distribution of the fissile material given that the composition and system size are determined. Although CLS w/ memory method changes the distribution of the chord length from background to the inclusion, which in turn changes the inclusion distribution as discussed in Section 4, the total packing fraction of the inclusions, i.e. total mass of fissile material, does not change. This is why both CLS methods can predict the k_{eff} with the same accuracy. However, the average flux distributions calculated by the two methods differs significantly. In all the cases studied, the CLS w/o memory method predicts the flux much closer to the benchmark results than the CLS w/ memory method. It shows that the memory effect has strong influence on the spatial distribution of the flux. Contrary to k_{eff}, flux distribution is more sensitive to the spatial distribution of the inclusions than the mass conservation. Since CLS w/ memory method can cause a significant change in the distribution of the inclusion, compared to the benchmark configuration, the spatial flux distribution is changed considerably. Such a change becomes more appreciable as the scattering is made stronger in the background material due to more frequent backscattering events, which can be seen from comparing cases 1 and 2 with cases 3 and 4. Since memory effect is closely related to the scattering cross section in background material instead of inclusion materials, the difference in flux distribution between CLS method and benchmark is not changed significantly when the scattering cross section in the inclusion becomes stronger.

A careful observation on the flux distribution from CLS w/o memory method shows that it is very close to the benchmark result but still with a tiny difference. This can be related to the boundary effect studied in Section 3. CLS method tends to increase the inclusion packing fraction near the boundary region while having a slightly lower packing fraction than the benchmark in the internal region. This may cause the slight difference in the flux distributions between the benchmark and CLS simulations.

To cite this article: Chao Liang & Wei Ji (2011): On the Chord Length Sampling in 1-D Binary Stochastic Media, Transport Theory and Statistical Physics, 40:5, 282-303

To link to this article: http://dx.doi.org/10.1080/00411450.2011.639432

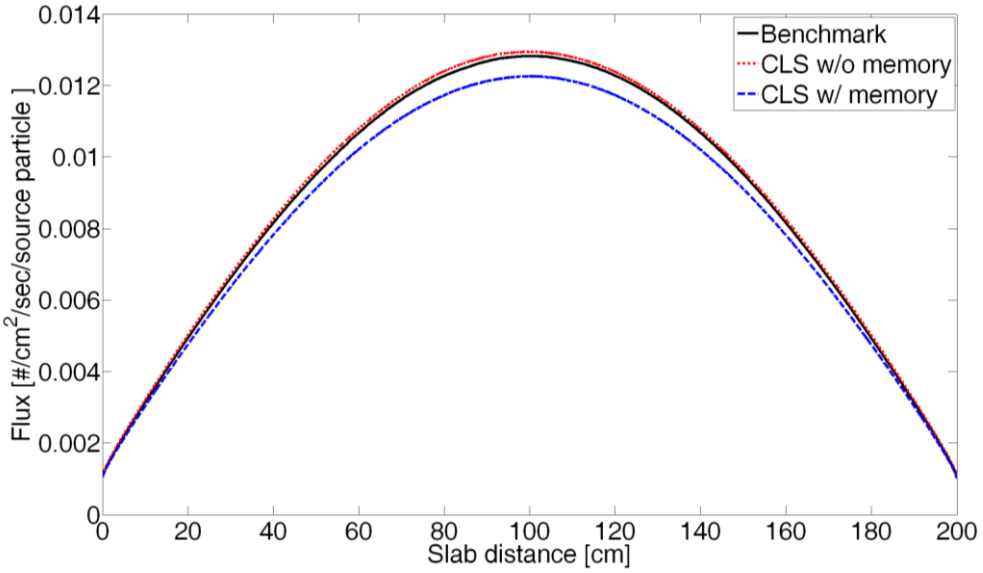

(a) Flux distribution comparison in case 1: low scattering cross section in background and low scattering cross section in inclusions

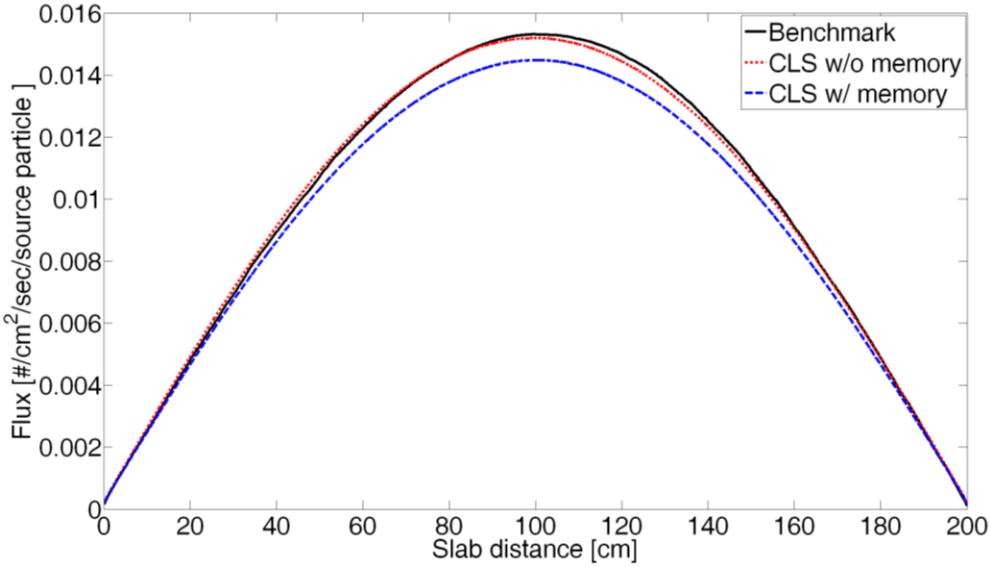

(b) Flux distribution comparison in case 2: low scattering cross section in background and high scattering cross section in inclusions

To cite this article: Chao Liang & Wei Ji (2011): On the Chord Length Sampling in 1-D Binary Stochastic Media, Transport Theory and Statistical Physics, 40:5, 282-303

To link to this article: http://dx.doi.org/10.1080/00411450.2011.639432

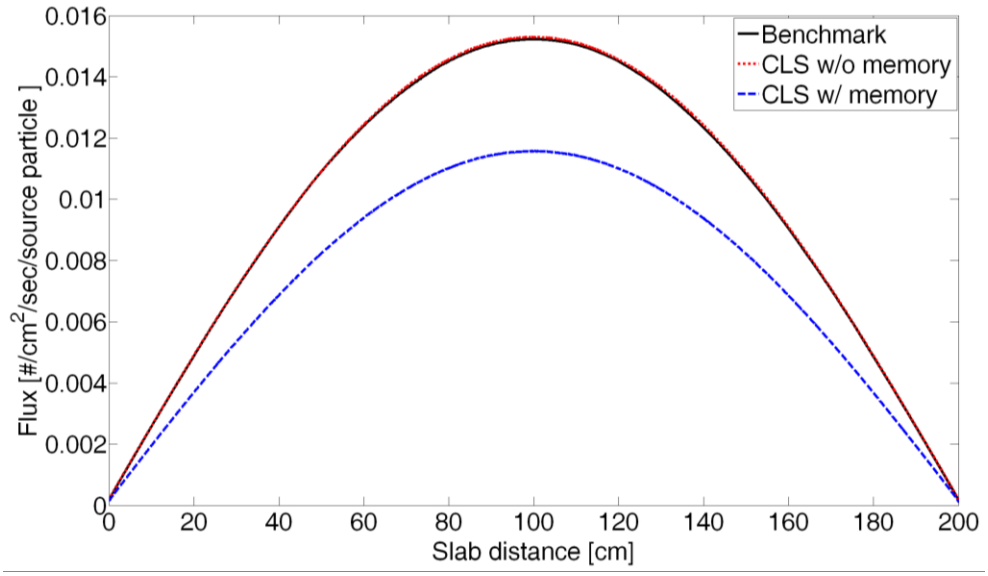

(c) Flux distribution comparison in case 3: high scattering cross section in background and low scattering cross section in inclusions

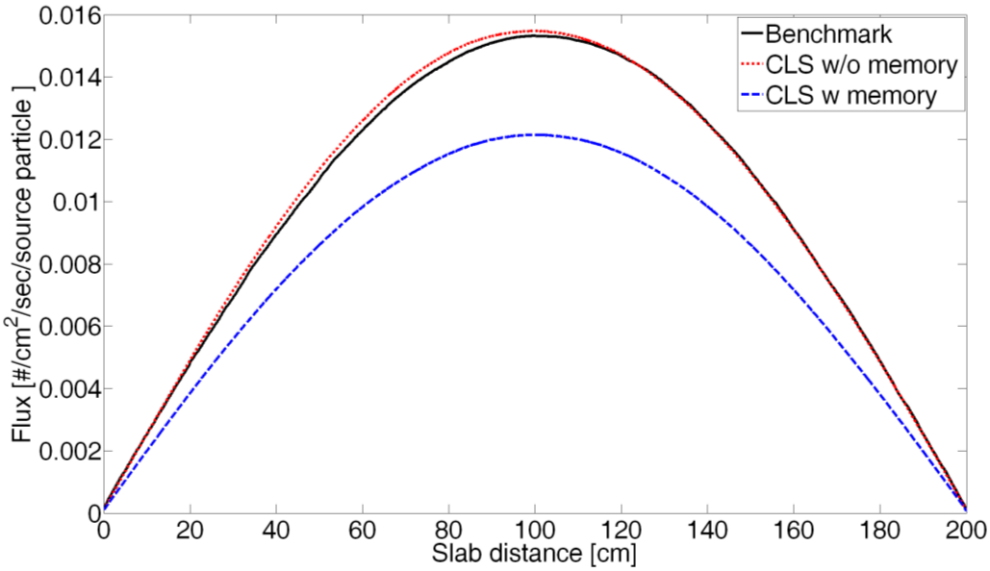

(d) Flux distribution comparison in case 4: high scattering cross section in background and high scattering cross section in inclusions

FIGURE 6 Flux distribution comparisons between Monte Carlo benchmark and CLS methods in eigenvalue problems

6. Conclusions

The impacts of the boundary and memory effects on the accuracy of the CLS method have been investigated in this paper. By applying CLS to solve fixed source and eigenvalue problems

To cite this article: Chao Liang & Wei Ji (2011): On the Chord Length Sampling in 1-D Binary Stochastic Media, Transport Theory and Statistical Physics, 40:5, 282-303

To link to this article: http://dx.doi.org/10.1080/00411450.2011.639432

in a 1-D random medium, it is demonstrated that both effects would affect the distribution of the inclusions in the medium so as to change the radiation behavior.

The boundary effect can cause a considerably higher local volume packing fraction for the inclusions at the region near the system boundary and a slightly lower packing fraction at the deeper region in the system, than the packing fraction in the benchmark configuration. This directly results in the change in reflection rate at the radiation incident boundary and the flux distribution inside the system. This has been demonstrated in the fixed source problem. This change would become obvious as the scattering cross section increases in the inclusions.

The memory effect can cause the change in the statistical characteristics of the system configuration depending on whether or not the radiation particle remembers the last inclusion that it has just left. It is demonstrated that the CLS w/o memory method can produce more accurate solutions than the CLS w/ memory method. This accuracy systematically holds for a series of scenarios in fixed source and eigenvalue problems studied in this paper.

Although the above conclusions are made under the 1-D random media configuration, it is expected that the same impacts from the boundary and memory effect can be observed in 2-D (disks randomly distributed in a background region) or 3-D (spheres randomly distributed in a background region), and the only difference is to what extent these impacts have on the accuracy of the CLS method.

Acknowledgements

This work was performed under the auspices of the U.S. Nuclear Regulatory Commission Faculty Development Program under contract NRC-38-08-950.

References

Brantley P.S. (2011). A benchmark comparison of Monte Carlo particle transport algorithms for binary stochastic mixtures. *J. Quant. Spectrosc. Radiat. Transfer* 112:599-618.

Donovan T.J., Danon Y. (2003). Application of Monte Carlo chord-length sampling algorithms to transport through a two-dimensional binary stochastic mixture. *Nucl. Sci. Eng.* 143:226-239.

Donovan T.J. et al. (2003). Implementation of chord length sampling for transport through a binary stochastic mixture. *Proceedings of the nuclear mathematical and computational sciences: a century in review, a century anew*, Gatlinburg, TN, April 6–11, 2003 [on CD-ROM].

To cite this article: Chao Liang & Wei Ji (2011): On the Chord Length Sampling in 1-D Binary Stochastic Media, Transport Theory and Statistical Physics, 40:5, 282-303

To link to this article: http://dx.doi.org/10.1080/00411450.2011.639432

Griesheimer D.P. et al. (2011). Analysis of distances between inclusions in finite binary stochastic materials. *J. Quant. Spectros. Radiat. Transfer* 112:577-598.

Ji W., Martin W.R. (2007a). Monte Carlo simulation of VHTR particle fuel with chord length sampling. *Proceedings of the joint international topical meeting on mathematics & computation and supercomputing in nuclear applications (M&C+SNA2007)*, Monterey, CA, April 15–19, 2007 [on CD-ROM].

Ji W., Martin W.R. (2007b). Determination of chord length distributions in stochastic media composed of dispersed microspheres. *Trans. Am. Nucl. Soc.* 96:467-469.

Ji W., Martin W.R. (2008). Application of chord length sampling to VHTR unit cell analysis. *Proceedings of the international conference on the physics of reactors (PHYSOR 2008)*, Interlaken, Switzerland, September 14-19, 2008 [on CD-ROM].

Murata I. et al. (1996). Continuous energy Monte Carlo calculations of randomly distributed spherical fuels in high-temperature gas-cooled reactors based on a statistical geometry model. *Nucl. Sci. & Eng.* 123:96-109.

Murata I. et al. (1997). New sampling method in continuous energy Monte Carlo calculation for pebble bed reactors. *J. Nucl. Sci. Tech.* 34:734-744.

Reinert D.R. et al. (2010). Investigation of stochastic radiation transport methods in binary random heterogeneous mixtures. *Nucl. Sci. Eng.* 166:167–174.

Torquato S. (2002). *Random Heterogeneous Materials: Microstructure and Macroscopic Properties*. Springer-Verlag, New York.

Widom B. (1966). Random sequential addition of hard spheres to a volume. *J. Chem. Phys.* 44:3888-3894.

Zimmerman G.B., Adams M.L. (1991). Algorithms for Monte-Carlo particle transport in binary statistical mixtures. *Trans. Am. Nucl. Soc.* 64:287-288.